Phase dissolution and improving properties of completely decomposed granite through alkali fusion method

Jean-Baptiste Mawulé Dassekpo[a,*], Lixin Miao[a], Jing Bai[b], Qianyi Gong[c], Ning Ning Shao[c], Zhijun Dong[c], Feng Xing[b,d], Jianqiao Ye[e,*]

[a]*Tsinghua Shenzhen International Graduate School, Research Center for Modern Logistics, 518055, China.*
[b]*College of Civil and Transportation Engineering, Shenzhen University, 518060, China.*
[c]*Institute of Technology for Marine Civil Engineering, Shenzhen Institute of Information Technology, 518172, China.*
[d]*Guangdong Provincial Key Laboratory of Durability for Marine Civil Engineering, Shenzhen University, Shenzhen, 518060, China*
[e]*Department of Engineering, Lancaster University, Lancaster, LA1 4YR, UK*

Corresponding authors email: dassekpo.jb@gmail.com; j.ye2@lancaster.ac.uk

Abstract

Low-reactive completely decomposed granite (CDG) was successfully synthesized by thermal activation with the addition of NaOH at low alkali/CDG mass ratio of 0.1/1. During alkali fusion, the degree of amorphicity of CDG rich in kaolinite ($Al_2Si_2O_5(OH)_4$) increased and a significant reduction of the peak intensities occurring between 20 and 45 (^{o}2 theta) was observed. Reactivity analysis indicated that, initial CDG requires high molar NaOH to provide a proper dissolution, whereas fused CDG exhibits high reactivity (^{29}Si = 555.57 ppm; ^{27}Al = 223.73 ppm) at low NaOH concentration. Moreover, results from the setting time, varied between 15-45 min, indicating that alkali fusion is very effective for improving the dissolution of the fused CDG under Na_2SiO_3 solution. However, the setting time decreases as the reaction degree accelerates. FTIR analysis of the fused CDG presented lower wavenumber band of around 975 cm^{-1}, confirming a decline of crystalline phases. In addition, SEM-EDS characterization and alkalinity analysis showed a compactness of the structure due to the liberation of enough sodium aluminosilicate gel. Finally, results from the mechanical test (4.75-39.55 MPa) and water solubility inferred that, by enhancing the reactivity of CDG by alkali fusion and by addition of up to 15% GGBS, CDG can be optimally recycled as an alternative source material to produce geopolymers.

Keywords: Completely decomposed granite; Alkali fusion; Dissolution; Reactivity; Setting time; Alkali-activated binder.

1. Introduction

Completely decomposed granite (CDG) is a natural material distributed worldwide and abundantly used for slopes deformation and stability, walls retaining, excavations, foundations and subgrade works [1]. The amount of CDG waste is very high especially in developing nations or cities due to the large numbers and scales of constructions projects, a phenomenon exacerbating environmental pollution and degradation. An expansion in the volume of CDG in Shenzhen city (South China) is seen as a result of numerous infrastructure projects initiated by the local government, and it is the main cause of the landslide observed in the city some years ago [1, 2]. In fact, according to the Bureau of Housing and Urban Development, 36148 million cubic meters of construction waste was generated in Shenzhen city from 2016 to 2019. However, only 2441 million cubic meters were recycled and utilized [3]. In a framework of the project titled "Shenzhen Residual Waste Acceptance Site Special Plan (2011-2020)", the Bureau projected an average annual generation of waste for each construction project from 2018 to 2035. From the 8 types of construction projects, evidently granitic waste ranked first at 7084.0 million cubic meters, then demolition waste at 2037.3, renovation waste at 645.0, construction waste at 495.4 and finally mud at 198.3 million cubic meters [3]. Accordingly, the construction waste distribution figures showed that about 70% of generated wastes are granitic waste, and as such recycling CDG waste is necessary for the protection of the environment.

CDG, like other residual soils, varies in its properties depending on both the parent rocks and the degree of weathering. According to the Geotechnical Engineering Office (GEO) [4], there are six types of granites, namely: fresh granite, slightly weathered granite, moderately weathered granite, strongly weathered granite, completely decomposed granite (CDG), and granite residual soil. The granites are classified contingent to their respective weathering levels. In the case of CDG

granites, the parent rock decomposes completely, with some traces of the parent rock fabric and texture being visibly noted. Less attention has been given to the evaluation of mechanical and physical performances of CDG in geopolymer technology except for a few studies on its properties as fine aggregates [5]. The studies on CDG's properties as fine aggregates, developed direct and triaxial shear experimental tests and concluded that a decrease in the percentage of fine aggregates will decrease cohesion, on one hand, and increase internal friction angle, on the other. The outcome of the direct shear results also proved that soils comprising lower quantities of fine aggregates have much lower strength [5]. Zhao et al. [6] conducted multi-phases loading and unloading triaxial tests to study the mechanical and deformation behaviors of intact CDG. The tested CDG samples revealed a linear-elastic trend in the first cycles, followed by accumulated plastic deformations during the remaining loading and unloading sequences. Furthermore, within three and four loading cycles, the stress-strain curves showed fragile failure whiles the peak shear strength decreased. In the same perspective, Wang et al. [7], while researching on the fines content effect on dynamic compaction grouting, noticed that the compaction of CDG expanded with swelling fines content, and that the fines could reach peak compaction efficiency at a certain percentage. To valorize CDG in geopolymer technology, Dassekpo et al. [1] equally showed that the inclusion of partial volume of fly ash can increase the compressive strength of CDG waste. According to that study, the optimal strength of CDG combined with fly ash paste could be achieved at an early time, however the full CDG strength kept on increasing over time.

In addition to the valuable benefits of CDG particles distribution, considering the amount of alumina and silica oxides, it is likely to increase its low reactive phase and performance through alkali fusion for its effective use in geopolymer production. Geopolymer is an emerging technology which offers potential conversion of solid industrial wastes into greener cements. SiO_4

and AlO_4 elements make up geopolymer materials which are poly-condensed in a high alkali solution environment to form three-dimensional structures with stabilized power given by alkaline earth ions [8]. It offers appealing application opportunities and exhibits good resistance, excellent chemical and physical properties, optimal and long-term durability, and more importantly, low cost and low energy consumption [9, 10]. Apart, the energy consumption required for the production of geopolymer, especially the manufacturing of alkali activators, its energy consumption is in some cases lesser than that required in the production of Ordinary Portland Cement (OPC). Moreover, the production of geopolymer binders can provide 80% or greater carbon-dioxide (CO_2) emission reduction compared to the production of OPC [11]. Several minerals, industrial by-products and wastes, such as fly ash [12], slag [13], Biochar-red clay [14], clay-waste [15], loess [16], granite quarry dust [17], and stone cutting waste [18] have been used successfully and their applicability in geopolymer synthesis has been proven. The common peculiarity of these industrial wastes is that they all contain, in amorphous form, high amount of silica (SiO_2) and alumina (Al_2O_3) that react with alkali solutions under normal or elevated temperatures through the geopolymerization process [9, 19]. The hardening of geopolymer can be achieved at ambient temperature or moderately high temperatures below 100^{o}C, relying on the level of responsiveness of the initial precursors. However, one issue with this ordinary procedure is that some alumina and silica rich materials reach low levels of reactions because of their mineralogical composition, normally comprising of high crystallized minerals [20]. To overcome this drawback, researchers developed and used a method called alkali fusion to successfully upgrade the responsiveness of various ash source materials [21-23]. The method consists of alkali pre-activation of low reactive raw materials and sodium hydroxide by heating through calcination at temperatures higher than the melting point of NaOH. The reason of using NaOH as well as

applying fusion was to increase the yield of zeolites by dissolving more silicates and aluminosilicates from raw materials [24]. After alkali fusion, sodium silicate solution was used to activate the ash of the grounded fused materials. The resultant geopolymer showed high degree of reaction, and as such, an improved mechanical strength and fast setting time. [21, 25, 26].

In light of the foregoing, this study examined the prospect of using completely decomposed granite (CDG) as the only aluminosilicate raw material or its combination with other supplementary materials in the synthesis of alkali-activated binders by applying alkali fusion method. The natural state of CDG, as well as the fused CDG and the supplement ground granulated blast slag (GGBS) were characterized by X-ray fluorescence (XRF) and their mineralogy changes by X-ray diffraction (XRD) were analyzed. To assess the readiness of Si and Al elements contained in CDG solid waste for dissolution, inductively coupled plasma mass spectrometry, Thermo Scientific iCAP RQ (ICP-MS) was utilized to examine the reactivity phase of CDG under different NaOH molarity. Thereafter, the initial CDG, fused CDG and supplementary proportion of 5, 10, 15% GGBS added into the fused CDG were used as aluminosilicate source in the manufacture of geopolymer pastes and mortars cured under different thermal conditions. The setting time of the developed CDG pastes were tested using Automatic Vicat Apparatus, SME-WKY1000 (SHIMAI Instrument). FTIR Spectrometer (Spectrum 100, Perkin Elmer) was used to identify functional groups of CDG. Also, the structural analysis by SEM as well as the alkalinity examination using EDS of the resulted CDG geopolymers were undertaken. The hardened CDG geopolymer performances were determined by compressive and split tensile strengths and water durability after several days of immersion was conducted to evaluate the gel formation in the CDG mortars. Finally, details and specific applications of the developed material were highlighted and discussed.

2. Materials and testing method

2.1 Materials

The CDG examined was sourced and collected from construction site of Shenzhen-Longang Metro line. To prepare the materials, the collected CDG were cleaned first to remove industrial waste and then dried at 105^{o}C for a day in order to reduce any water content before they were sieved. Ground granulated blast slag (GGBS) sourced from Henan Province (China) was then used as partial replacement in the mixture. CDG geopolymer pastes were prepared for the material characterization and fine river sand was added to the mixture to synthesize geopolymer mortars. In the synthesis process, sodium silicate (Na_2SiO_3) with SiO_2/Na_2O of 1.5 was utilized.

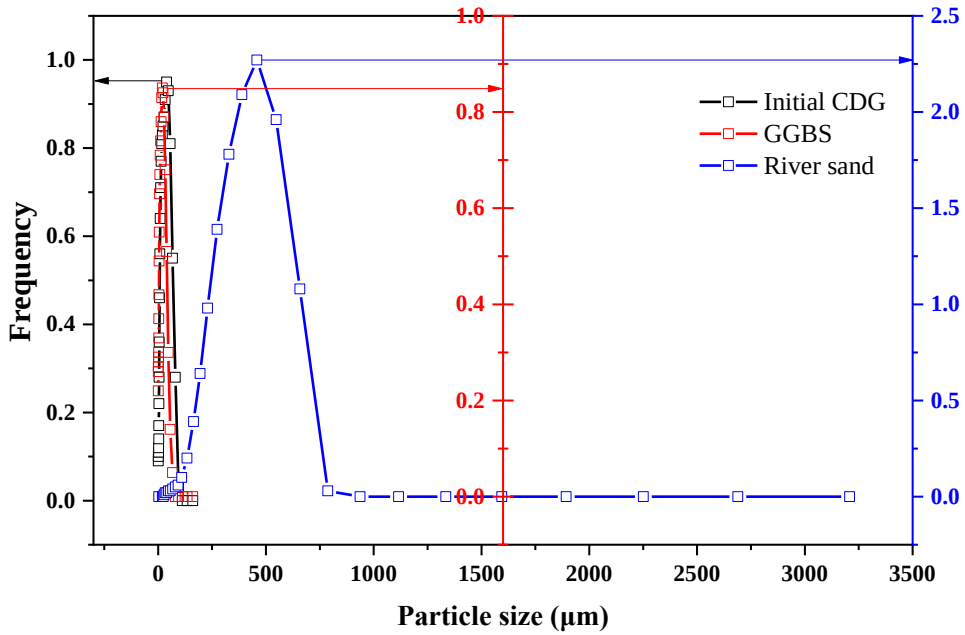

Fig. 1 Particle size distribution of initial CDG, GGBS and river sand

Laser Granulometer Helos (Sympatec GmbH) was employed for particle size distribution (PSD) of both precursors and sand and the results are showed in Fig. 1. The PSD rate of the initial CDG ranges between 0.1 to 1.0 and varies from 0.2 to 0.9 for GGBS. The river sand material was comprised of major particles with rate between 0.0 to 2.5. BET Surface Area and Porosity Analyzer,

ASAP 2460 (Micromeritics) were used to determine the Specific surface areas (SSA) of initial and fused CDG, and GGBS. The results were at about16.65 m^2/g for initial CDG, 20.93 m^2/g for fused CDG and 15.96 m^2/g for GGBS. Using Le Chatelier, specific gravity of the raw materials was also examined, and the result considered. The specific gravity of the initial and fused CDG was found to be equal to 2598.21 kg/m^3 and 2243.95 kg/m^3 respectively, and for GGBS is around 2752.30 kg/m^3.

2.2 Testing method

2.2.1 Alkali fusion procedure

Dried fine grains of CDG waste were blended with pellets of NaOH at a lower alkali/CDG mass ratio of 0.1/1 in a ball mill for 15 min. This ratio was chosen based on preliminary tests aiming to minimize as much as possible the quantity of NaOH in a more reasonable volume of CDG. The resulting mixtures were heated at 650°C in an electric furnace for a period of 2 hours at a heating rate of 30°C/min. Fused CDG was cooled by gradually decreasing the furnace set temperature to 30°C. After cooling, the fused CDG was grounded in the ball mill for another 15 minutes to acquire a homogenous blend. The initial and fused CDG, as well as the supplement GGBS were examined under X-ray fluorescence (XRF, Thermo Fisher ARL Perform'X) to determine the chemical composition of the raw materials and to estimate the influence of alkali fusion on the composition of CDG (Table. 1).

Table 1 Chemical composition of initial CDG, fused CDG and GGBS

Element as oxide	Initial CDG	Fused CDG	GGBS
SiO_2	52.49	45.77	34.38
Al_2O_3	37.55	35.80	20.60
CaO	0.498	0.288	30.75
Fe_2O_3	4.540	4.230	0.690
K_2O	3.320	2.740	0.470
TiO_2	0.411	0.450	0.520
Na_2O	0.092	10.02	0.610
MgO	0.550	0.357	9.980

MnO	0.044	0.048	0.150
P_2O_5	0.067	0.042	0.060
SiO_2/Al_2O_3	1.397	1.278	1.668
LOI: Loss on ignition	8.840	9.520	9.890

2.2.2 Synthesis of CDG geopolymers

To produce the geopolymer mortar samples, the blends of initial raw CDG, fused CDG and fused CDG combined with different ratios of 5, 10 and 15% GGBS were mixed with Na_2SiO_3 solution having a SiO_2/Na_2O molar ratio of 1.5. For all the configurations, the liquid solid ratio (L/S) was kept at 1/1.2 and a fine aggregates binder ratio (A/B) of 2.75/1 was applied. Samples containing initial CDG and fused CDG were labeled IC00 and FC00, and those with partial addition of 5, 10 and 15% GGBS in the fused CDG were labeled FC05, FC10, FC15, respectively. The mix composition of each sample is summarized in Table 2.

Table 2 CDG geopolymers mix design ratios

CDG mortars	CDG/GGBS	Alkali/CDG	L/S	A/B
IC00	100/0	-	1/1.2	2.75/1
FC00	100/0	0.1/1	1/1.2	2.75/1
FC05	95/05	0.1/1	1/1.2	2.75/1
FC10	90/10	0.1/1	1/1.2	2.75/1
FC15	85/15	0.1/1	1/1.2	2.75/1

To prepare the geopolymer mortars, the measured dry initial and fused CDG powders and GGBS were mixed in a rotating pan mixer for 5 minutes. The sodium silicate (Na_2SiO_3) liquid was then added in and also mixed for 5 minutes, followed by mixing sand, as fine aggregates to the pastes for another 5 minutes [27]. To remove entrapped air, the fresh mortar was placed in a 70 x 70 mm plastic mold and compacted on a vibrator plate for 2 – 3 minutes. Three cubes were made ready for testing each variable. At room temperature, the sealed samples were allowed to rest for 4 hours. The samples were then removed from the molds after the resting time has elapsed. Fig. 2 shows the entirety of the preparation process of the geopolymers. Two curing methods were used

in this study. The first one was to cure the samples at an elevated temperature of 70°C with relative humidity of 50%RH for 24 hours before exposing samples to the open air to dry at room temperature until the testing time. The second method involved curing the samples directly at ambient environment until they were tested. The use of these two methods were to study the effect of a short period of elevated temperature on the degree of reaction of the materials.

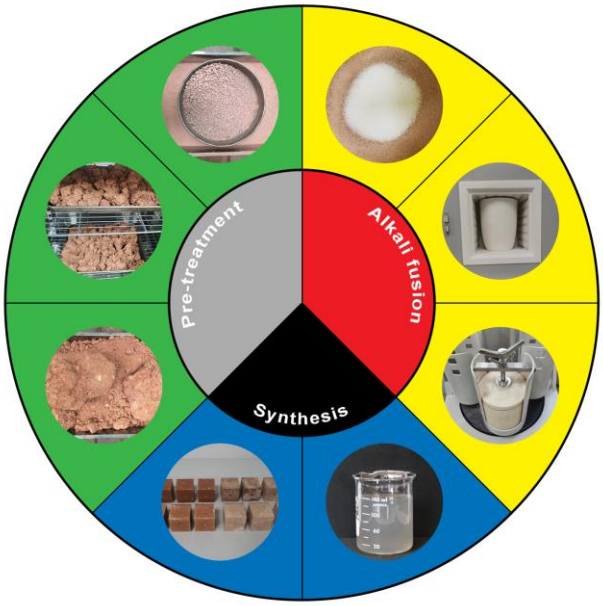

Fig. 2 Manufacturing process of CDG geopolymers

2.2.3 Reactivity phase analysis

To evaluate the influence of the alkali fusion on CDG reactivity, a comparative dissolution study on the reactive phase amount was undertaken on the initial and fused CDG. A weight of 0.5 g of each powder specimen was dissolved in 20 mL NaOH solution with 2 different molar (8M and 10M) ratios. The solution was magnetically stirred for 2 hours with 1000 rpm at room temperature. Thereafter, the residue was filtrated through 0.22 μm syringe filter and diluted with purified water and then the solution was collected. Inductively coupled plasma mass spectrometry, Thermo Scientific iCAP RQ (ICP-MS) was used to examine the resultant solution and the

reactivity during geopolymerization was assessed by the dissolution extents test of Si and Al elements from the solid CDG.

2.2.4 Experimental procedure

The chemical composition of the raw materials was conducted and analyzed by X-ray fluorescence (XRF, Thermo Fisher ARL Perform'X). The initial and fused CDG mineralogy was studied using X-ray diffraction (XRD, D8 Advance), and the reactivity of both CDG mixtures during geopolymerization were assessed by the dissolution extents test of Si and Al elements using ICP-MS, as described in section 2.2.3.

Prior to the preparation of mortar, the setting time of the fresh CDG pastes were measured using Automatic Vicat Apparatus, SME-WKY1000 (SHIMAI Instrument), and the observations were recorded. The diameter of the needle measured about 1.13 ± 05 mm and its flat length about 50 ± 1 mm. The internal diameter of vicat mould measured about 70 ± 5 mm at the top and 80 ± 5 mm at the bottom, and was of a height of 40 ± 0.2 mm.

Using a Perkin Elmer, FTIR Spectrometer (Spectrum 100) with frequency range of 4000-650 cm^{-1}, an infrared spectroscopy analysis was undertaken to identify the functional group of CDG. During the experiment, the middle layer of every paste of about 5–10 mm was collected, and small amount of powder was tested at constant temperature.

Microstructural aspects and chemical composition of the tested CDG samples were undertaken by SEM-EDS, employing Zeiss Gemini 300 X-MAXN, Microanalysis Oxford Instruments. The compressive and split tensile strengths performances of the CDG geopolymer mortars were obtained on CRIMS load testing machine, whereas water permeability was performed by simple immersion test to evaluate the gel formation in the CDG geopolymer mortars.

3. Results and discussion

3.1 Characterization of initial and fused CDG

The outcome obtained from the initial CDG, fused CDG and GGBS using the X-ray fluorescence method presented a high proportion of SiO_2 at 52.49%, 45.77%, 34.38% and Al_2O_3 against 37.55%, 35.80%, 20.60%, respectively. Other compounds including CaO, Fe_2O_3, K_2O, TiO_2, Na_2O, MgO, MnO, P_2O_5 are equally present. A 4.54% Fe_2O_3 in the initial CDG indicated the existence of biotite, likely associated with an additional phyllosilicate ferric aluminosilicate minerals. The amalgamation of K_2O and Na_2O at 3.32% and 0.092%, respectively, at the natural state of CDG suggests the existence of K/Na-feldspar minerals, with the proportion of K_2O likely related to the K-feldspar minerals. The high percentage of Na_2O (10.02%) in the fused CDG can be attributed to the addition of sodium hydroxide (NaOH) during the alkali fusion process. Moreover, a high amount of CaO (30.75%) and MgO (9.98%) was found in GGBS, which is not surprising, as it was proved that GGBS is a glassy and granular material mainly composed of SiO_2, CaO, Al_2O_3 and MgO.

The XRD patterns of the initial (I-CDG) and fused CDG (F-CDG) are presented in Fig. 3. As shown in Fig. 3 (a), kaolinite ($Al_2Si_2O_5(OH)_4$) was the dominant mineralogical phase in I-CDG. Other secondary minerals such as quartz (SiO_2), muscovite ($KAl_2Si_3AlO_{10}(OH)_2$) and dickite ($Al_2Si_2O_5(OH)_4$) were also identified. An indication that the minerals contained in initial CDG are highly crystallized was noticed from the shape of the pattern showing the range of the peaks and intensity. An important crystallization phase is the degree of crystallization with no wide jump between 20 to 40^o (^{o}2 theta).

XRD pattern of the fused CDG is shown in Fig. 3 (b). The differentiation between I-CDG and F-CDG clearly indicates the modification of the mineralogical composition of CDG by alkali

fusion. XRD pattern of F-CDG also presents an important lessening of peak intensities compared to I-CDG, and an increase in Na_2O amount, a phenomenon attributable to the transformation of CDG from crystalline to amorphous phase in presence of NaOH. The Na-rich phase observed in the fused CDG results from decomposition of the initial aluminosilicate minerals contained in CDG solid, more precisely, the release of SiO_4 and AlO_4 tetrahedrons accomplished by–OH groups during the fusion process [28] and the amalgamation with the Na^+ free sodium ion from sodium hydroxide. When the temperature of such solution is raised to 318^{o}C, the above reaction generally occurs, at which NaOH melts and becomes ionized at a limited extent in the state of flux [29]. An indication of the number of unbound Na^+ in the structure was illustrated by the high peaks in intensity of the sodium silicate, which will react easily at the silicate level. By observing the XRD pattern of the fused CDG, it can be showed that between 20 and 45 (^{o}2 theta), there is a small broad hump, indicating the change of crystallinity into amorphous phase. From these results, it can be deduced that the alkali fusion method has great impact on CDG structure. It is important to emphasize that though it is recommended to use XRD and XRF in evaluating amorphous components of aluminosilicate materials, how quickly these components are ready for dissolution cannot be shown [30]. It is for this purpose that dissolution test was applied in this research to evaluate the consequence of alkali fusion on the synthesis reaction of CDG.

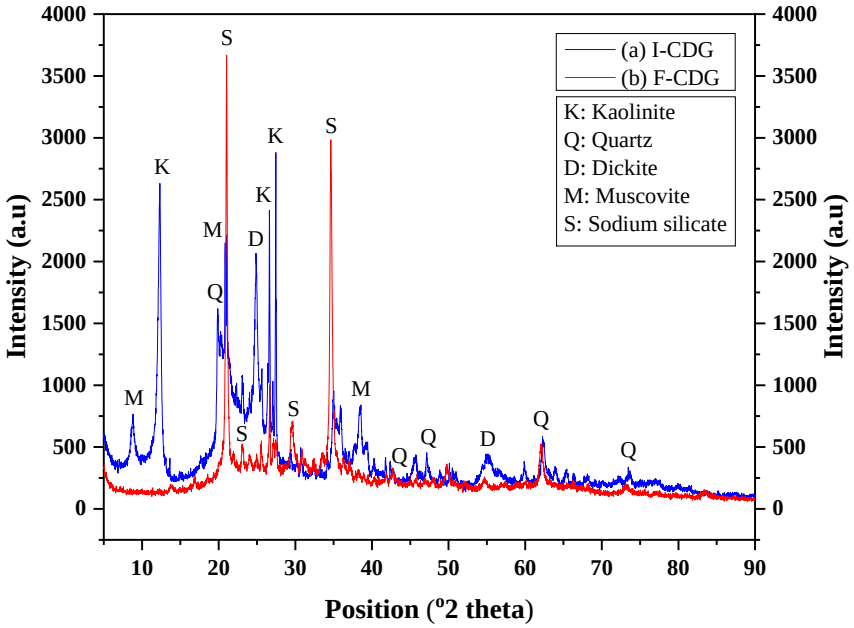

Fig. 3 XRD patterns of: (a) initial CDG, (b) fused CDG

3.2 Dissolution of initial and fused CDG

Geopolymerization is a very complex process that requires different reactions including dissolution, reorientation and solidification of Si and Al species from the precursors [31]. Thus, dissolving Si and Al elements from the solid primary material plays an important role in the geopolymerization process. Accordingly, the dissolution test was performed on the initial and fused CDG, the results of which, are presented in Fig. 4. It can be seen that, the dissolution of Si in the initial CDG presents 29.67 ppm for 8M NaOH and 98.28 ppm for 10M NaOH. As for the fused CDG, a range of 555.57 to 123.22 ppm was observed respectively for 8 and 10M NaOH solutions. Similarly, the dissolution of Al in the initial CDG varies from 17.60 ppm to 80.95 ppm, respectively, for 8 and 10M NaOH; and for the fused CDG, it varies between 223.73-63.45 ppm for 8 and 10M NaOH. The results show that, the initial CDG requires high molarity in the NaOH in order to provide a proper dissolution. The fused CDG, on the other hand exhibits high reactivity especially at low 8 Molar NaOH concentration and both reactive Si and Al species from fused CDG at 10 Molar NaOH molarity present low dissolution rates near those of initial CDG. This is

due to the initial addition dosage of NaOH pellets during the alkali fusion process and the physico-chemical modification. In other words, there was an increase of the level of amorphicity and change of structural aspects of the emanating silica and alumina solid from CDG under Na_2SiO_3 solution. From these results, it can also be concluded that fused CDG needs low molarity NaOH for the synthesis of alkali-activated binder.

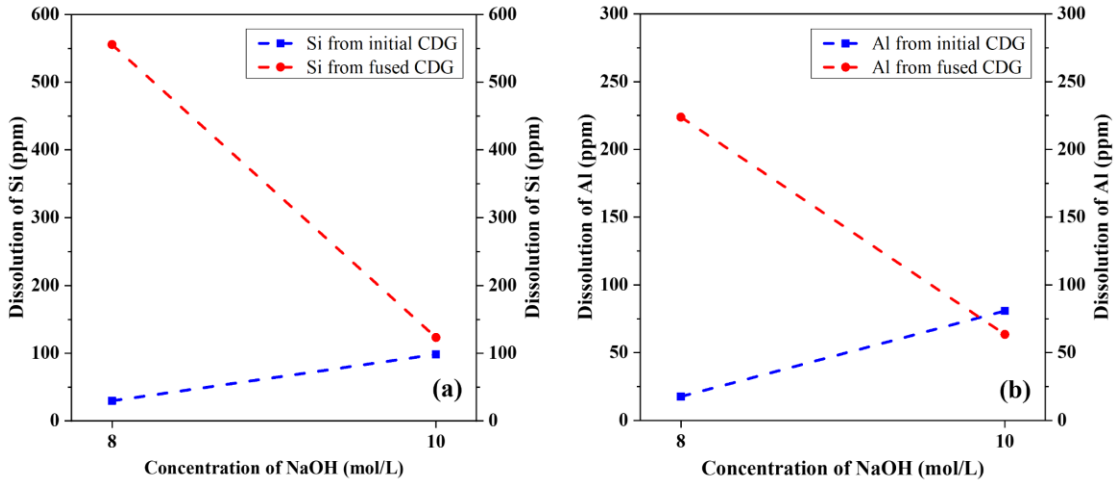

Fig. 4 Dissolution of Si and Al from initial and fused CDG

3.3 Setting time

Investigation on the setting time has been conducted on CDG pastes and the results are presented in Fig. 5. The setting time, in geopolymer, is an important parameter since it defines the associated practicalities, especially possible transport time and handling duration of the material. As showed in the figure, the setting time varied between 15 and 45 minutes. The tardy setting time of 45 min was observed in the initial CDG. From this result, an explanation as to why the dissolution of the initial CDG is lower would be: weak dissolution decreases the degree of polymerization and the hardening of the composite gel. The setting time of paste activated with fused CDG, on the one hand, presented 32 min, with a variance equal to 13 min, compared to the initial CDG, on the other. From this particular case, the setting time seems to be governed by the alkali fusion method as induced by the temperature conditioning and pre-addition of NaOH.

Moreover, the setting times of the fused CDG with partial addition of GGBS were equally recorded. The times varied between 24, 18 and 15 minutes against 5, 10, and 15% GGBS, respectively. By examining the setting time values obtained from the fused CDG and fused CDG with addition of GGBS, it is clear that the setting time continuously decreases and that the short setting time was observed only in the fused mixtures. This implied that, for the fused composition, the geopolymerization reactions are very short. Also, the addition of GGBS in the fused CDG is equally responsible of the reduction of the setting time. A larger volume of GGBS, lowers the setting time, i.e 15% supplementary GGBS reduces setting time to 15 min for fused CDG. This shows that the addition of GGBS into the fused CDG catalyzes the dissolution of Al and Si species, and consequently contributes to the formation of $[SiO(OH)_3]^-$ and $[Al(OH)_4]^-$, whose primary role is to enhance the polycondensation reaction and to form the polymeric binder [26]. From the foregoing observations and results, a deduction can be made that the alkali fusion method is very effective for promoting the dissolution and fast setting of the fused CDG. That notwithstanding, the setting time of fused CDG pastes decreases as the reaction degree accelerates.

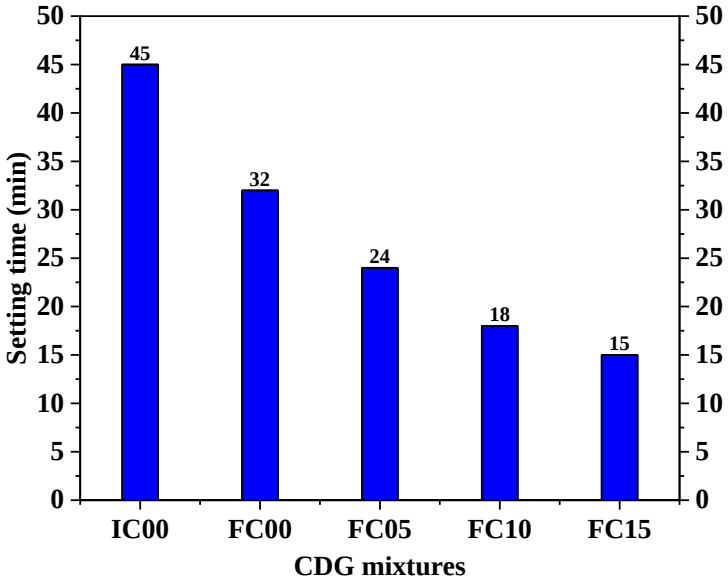

Fig. 5 Setting time of CDG geopolymer pastes

316
317 *3.4 FTIR analysis of CDG*

318 The spectra of the initial CDG, fused CDG and fused CDG with addition of 5, 10 and 15%
319 GGBS paste samples cured at 70ºC, 50%RH for 24 hours (denoted "HC") are presented in Fig. 6.
320 It can be observed that the spectra of the initial CDG presents a maximum peak at 1005 cm^{-1},
321 attributable to the continuous change of interatomic distance along the axis of the bond between
322 Si–O–Si and Al–O–Si groups of the aluminosilicate source [32, 33]. The absorption band observed
323 in this mixture is also characterized by the trace of albite [34]. In addition, in this same band, a
324 peak at 3695 cm^{-1} was observed. This peak is characterized by the presence of kaolinite, affirmed
325 by the XRD result, and is mostly on account of the O-H stretching frequencies allied with hydroxyl
326 ions.

327 Alkali fusion has greatly influenced the functional group of CDG. Thus, the strong band
328 of 1005 cm^{-1} observed in the initial CDG has shifted to lower wavenumber band of around 975
329 cm^{-1} for the fused CDG, and subsequently decreased to 960, 965 and 968 cm^{-1}, respectively in the
330 case of 5, 10 and 15% GGBS in the fused CDG. The lower IR spectrum observed in the fused
331 CDG is associated with the elastic shaking of Si–O and Al–O categories, indicating a decline of
332 crystalline phases in the long term structure of the CDG , as well as the development of the
333 amorphous phases [35]. Throughout the alkali fusion, the Si-O-Si and Al-O-Si bonds remained
334 hydrolyzed, resulting in a rise in the number of non-bridging oxygen atoms in the structure. This
335 is a fact that can be established from the outcome obtained from the fused CDG, which presented
336 a band at 975 cm^{-1}, attributed to a symmetrical stretching of the Si-O and Al-O bonds in the SiO_4
337 and AlO_4 tetrahedra, respectively [32, 36]. As a result, the bonding between the tetrahedral units
338 TO_4, with T=Si, Al, evolves more into an ionic state and eventually the T-O bonds begin to
339 generate a very low molecular vibrational force. Thus, the Si-O-T asymmetric stretching

vibrational band shifts to a lower wavenumber [33, 35]. According to previous studies, the reactivity of the source materials as geopolymer active precursors can be enhanced by increasing the number of non-bridging oxygen and the amorphous phase quantity in the initial substance [28, 35]. Thus, the result obtained from the fused CDG mixture showed the reactive phase of the material during the geopolymerization process, which was proven by the dissolution test results.

It was also noticed that there was an intermediate peak on the left and right side of the band. The value of the peaks varied between 910-865 cm^{-1} and 1450-1448 cm^{-1}, respectively. It is clear that the highest wavenumber is found in the initial CDG mixture and the lowest in the fused CDG. The mixtures with an addition of 5, 10 and 15% GGBS in the fused CDG, on the other hand, accumulate a peak of around 800 cm^{-1} (including the fused CDG). This peak value can be attributed to the silica (SiO_2) wavenumber bands represented in the polymeric $(SiO_2)_n$ molecules as well as the bending vibrational mode of the Si-O-Si- bonds.

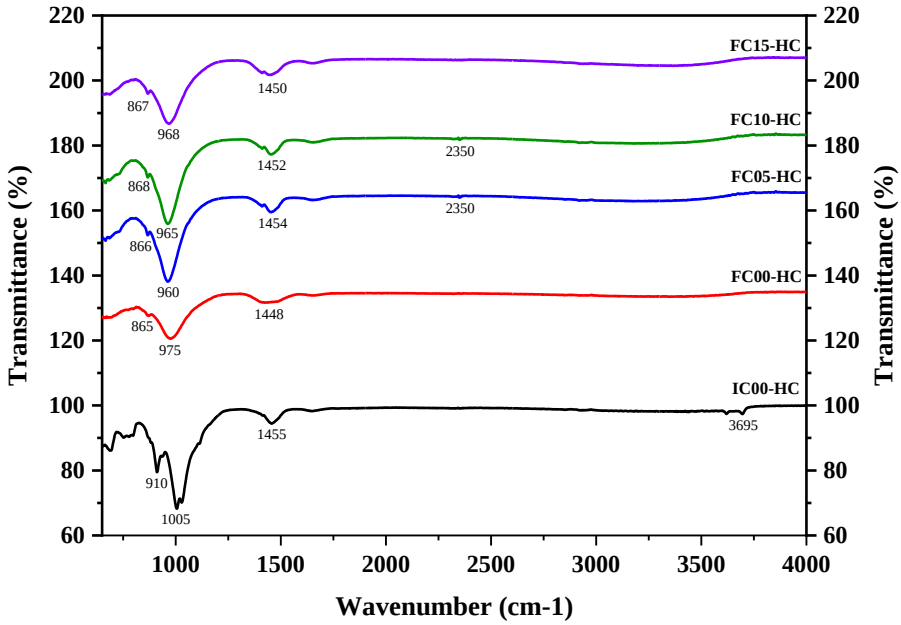

Fig. 6 FTIR spectra of CDG: IC00-HC=Initial; FC00-HC=Fused; FC05-HC=Fused CDG with 5%GGBS; FC10-HC= Fused CDG with 10%GGBS; FC15-HC= Fused CDG with 15%GGBS

3.5 Microstructural characterization

The SEM images at 28 days of the initial CDG, fused CDG and CDG with a variation of GGBS pastes cured under different conditions are presented in Figs. 7-8. In general, it can be seen that the alkali fusion method adopted, the curing conditions and the volume of the added GGBS have great effects on the microstructure of CDG. In the figures, the "HC", at the end of the labels denotes that the samples were subjected to a temperature of 70^{o}C for a period of 24 hours before being left in ambient temperature for the rest of the curing time; and those ending with "AC" are for the samples subjected to ambient temperature during the whole curing time.

Fig. 7 (a-b) shows the structure of the initial CDG geopolymer cured under different conditions. This structure is characterized by a heterogeneous and easily crumbled particles. This heterogeneity could be associated with the natural crystalline minerals and the weak dissolution at the natural state of the initial CDG, its particle size and shape. There has been evidence showing that usually the geopolymerization process happens around the surface of the aluminosilicate particles [37]. This aspect of the structure can also be justified by the fact that the initial CDG was only activated with sodium silicate (Na_2SiO_3). It is noteworthy that in geopolymer activation, a combination of NaOH and Na_2SiO_3 is generally utilized, and using Na_2SiO_3 solution only can lead to lower dissolution rate compared to that activated with OH^- compounds [38]. The microstructure of the fused CDG is also presented in Fig. 7 (c-d). It can be clearly observed that the fused CDG structure is more homogeneous. Some unreacted CDG particles with cracks are also visible on the surface, especially with the samples cured at ambient temperature only. This demonstrates that the alkali fusion and heating resulted in sufficient reactivity of the Al and Si from the initial CDG, which then raised the level of geopolymerization.

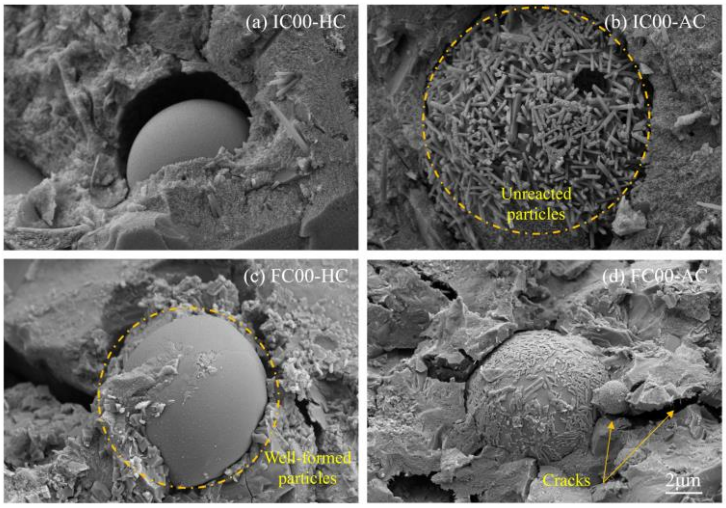

Fig. 7 SEM morphology: (a-b) Initial CDG, (c-d) Fused CDG

The fused CDG with an addition of 5, 10 and 15% GGBS microstructures are also contrasted, and the results are analyzed (Fig. 8 a-f). The general analysis of these three structures shows that the addition of GGBS has greatly influenced the microstructure of the CDG as the volume of GGBS increases, e.g., the compacity of the structure increases with less pores confirming the well-synthesized geopolymer structure. Also, alkali fusion of the samples with high reactive GGBS induces effective dissolution, better cohesion of the structure thereby enhancing the reaction and performance of CDG.

Most importantly, apart from the homogeneous structure recorded on most specimens, some superficial cracks were equally visible. Potentially, the cracks observed in most of the samples could be attributed to the use of sodium silicate solely in the activation. As earlier indicated when geopolymer is activated with soluble silicates into high level alkali concentration, the binder interference can promote greater interfacial bonding [39], which is a factor that favors cracks propagation in the material.

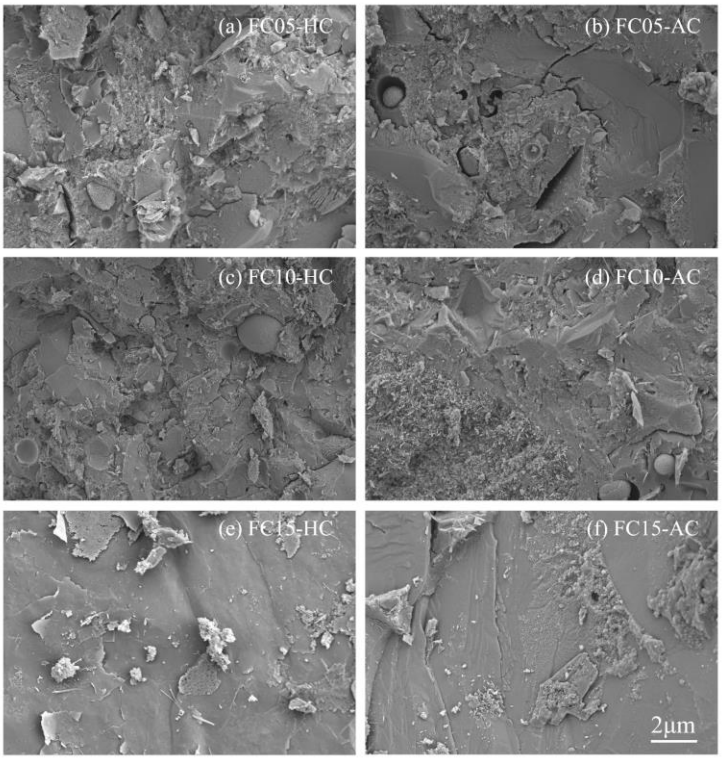

Fig. 8 SEM morphology: (a-b) Fused CDG + 5%GGBS, (c-d) Fused CDG + 10%GGBS, (e-f) Fused CDG + 15%GGBS

3.6 Alkalinity analysis by means of EDS

The elemental compositions, calculated Si/Al and Na/Al molar ratio of each CDG geopolymer paste samples from EDS are presented in Table 3. The fused CDG geopolymers have high percentage of Si/Al and Na/Al molar ratios of 6.14, 2.41 and 5.26, 2.32, respectively, for heat and ambient curing conditions. The high ratio demonstrates alkalinity of the fused CDG geopolymer, which releases a significant amount of Al from the solid CDG.

It is noteworthy that the geopolymerization process occurs in three different steps: i.e., dissolution of the alumina and silica rich precursor in $Si(OH)_4$ and $Al(OH)_4^-$ conditions, reorganization of the dissolved species and geopolymer network formation (Si–O–Si, Si-O-Al) of silicates and aluminates through polycondensation [20]. When the Na_2SiO_3 is added to the fused CDG, no specific dissolution occurs due to the liberation of $Al(OH)_4^-$ and $Si(OH)_4$ from the CDG initial materials after alkali fusion, thus leading leads to the next two steps of the

geopolymerization process. Accordingly, the two main phases of the formation of fused CDG are reorganization and polycondensation of the dissolved CDG species. The initial CDG undergoes the above-listed steps, thereby, presenting high concentration of Si and Al (66.38, 22.27 and 64.90, 24.31) with low concentration of Na (11.32 and 10.75), respectively, for heat curing and ambient curing.

It is pertinent to note that the Si, Al and Na elements in the fused CDG also present higher concentration, especially when GGBS was supplemented into the mixture. This observation can be attributed to the additional species from GGBS solid, and the higher Na is related to the prior addition of NaOH during the alkali fusion. Similarly, Ca element trace is also visible in the mixture and an increase can be observed as the percentage of GGBS increases in the fused CDG.

Table 3 Elemental analysis by means of EDS

		Element's concentration (Wt.%)				Molar ratio	
Samples	Curing	Si	Al	Na	Ca	Si/Al	Na/Al
IC00-HC	HC	66.38	22.27	11.32	0.03	2.98	0.50
IC00-AC	AC	64.90	24.31	10.75	0.04	2.66	0.44
FC00-HC	HC	64.24	10.45	25.23	0.08	6.14	2.41
FC00-AC	AC	61.22	11.62	27.00	0.16	5.26	2.32
FC05-HC	HC	62.23	24.42	12.82	0.53	2.54	0.52
FC05-AC	AC	62.12	16.79	20.89	0.20	3.69	1.24
FC10-HC	HC	57.47	22.93	17.26	2.34	2.50	0.75
FC10-AC	AC	56.11	21.88	19.00	3.01	2.56	0.86
FC15-HC	HC	55.86	17.90	21.68	4.56	3.12	1.21
FC15-AC	AC	53.58	18.98	21.71	5.73	2.82	1.14

**HC: 24h heat curing, AC: Ambient curing.*

The element distribution of FC15-HC sample at a specific surface is also presented in Fig. 9. It can be observed that the distribution of Si, Al, Na and Ca elements in the sample shows a majority homogeneous enrichment area. In general, it can be seen that all the elements are evenly distributed in the surface. This homogeneous distribution is a prove of the high extent degree of reactivity and the increase of the network connectivity in the formation of compact and high resistance CDG geopolymers.

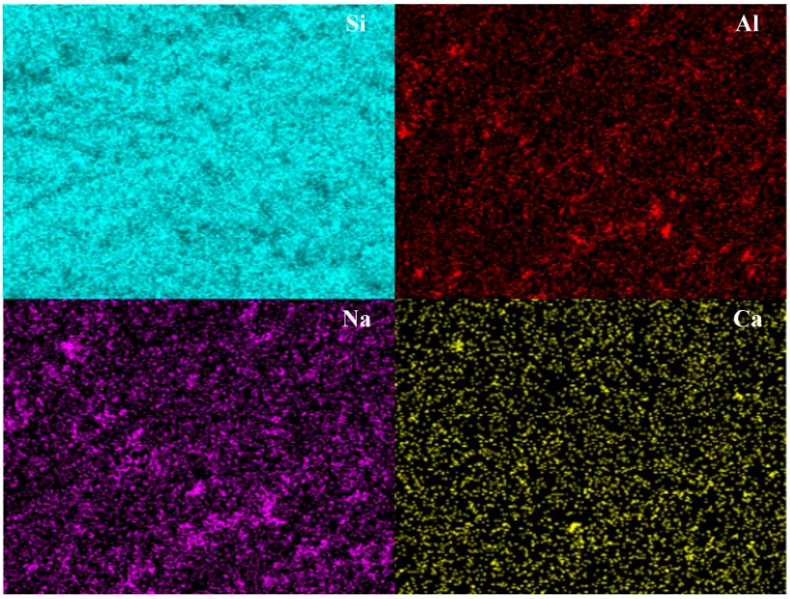

Fig. 9 EDS elemental distribution mapping of FC15-HC

3.7 Mechanical properties

Fig. 10 shows the average compressive and split tensile strengths of the CDG geopolymer mortars after undergoing a-28 days curing under different conditions including heating for 24 hours before ambient curing, and ambient curing only. The average compressive strength varies from 8.89 to 39.55 MPa for heat cured samples and varies between 4.75 to 30.21 MPa for the mixtures cured at ambient temperature (Fig 10 a). The strength improvements of the geopolymer mortars can be linked with different factors such as geopolymer gel (N–A– S–H) bonding strength, its type as well as the nature of the fine aggregates and the interfaces connection between the geopolymeric binder matrix and aggregates. All these factors are important in determining the geopolymer gel binding capability having a close relationship with the dissolution rate and reaction of the raw source material under alkali solution [39].

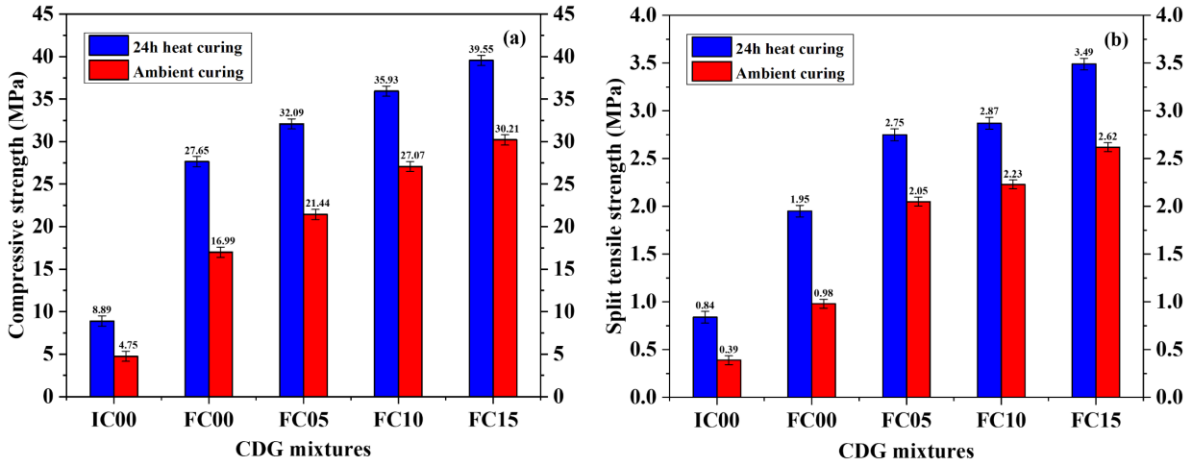

Fig. 10 Mechanical properties of CDG at 28 days curing:
(a) Compressive strength, (b) Split tensile strength

3.7.1 Effect of alkali fusion and curing method on CDG

The compressive strength of the initial and fused CDG geopolymer activated under 24 hours curing temperature are, respectively, 8.89 and 27.65 MPa at 28 days curing whereas samples cured at ambient temperature after 28 days exhibits lower strength of 4.75 and 16.99 MPa, respectively, for the initial and fused CDG geopolymer. The strength of the fused CDG geopolymer can reach up to 27.65 MPa and 16.99 MPa, respectively, for 24 hours heat curing and ambient temperature curing only. This affirms that fused CDG can be the only source material in for geopolymer system. The compressive strength evolution in both cases suggests that when CDG is used as aluminosilicate source material in the production of geopolymer mortars, an alkali fusion and few hours of heating is required to increase Si and Al dissolution rate, thus enhancing strength development. It is important to emphasize, however, that only sodium silicate (Na_2SiO_3) solution was used to activate all the mixtures in this study, including the initial CDG (IC00). The results were compared with those of the fused mixtures. The main reason for this choice is justified by the fact that the adopted alkali fusion method required pre-mixing CDG with NaOH and the fused mixtures were directly activated with Na_2SiO_3. Thus, this process also affects strength

development of the initial CDG, as demonstrated by the fact that sodium silicate activation alone could not provide the same strength as when it was used in combination with NaOH [38].

Beside the effects of the alkali solution and fusion method, it can also be seen that the 24 hours of heat activation similarly heightened the geopolymerization process. The samples cured at ambient temperature exhibits strength relatively inferior to those heat cured for 24 hours before submission to open air curing. Because of the foregoing, the importance of temperature in developing strength of CDG geopolymer is key. Its significance is showed in other aluminosilicate source materials; the temperature level and curing time play an important role in the final strength [19, 40, 41]. It is important to point out that the compressive strength obtained from the ambient cured samples, which varied between 4.75 to 30.21MPa, is still significant in the sense that the main aim of geopolymer technology is to reduce high-energy consumption materials with low-cost ones. The achieved strength of CDG obtained with ambient curing condition can find good applications in the construction sector. This follows the practice that suitable and applicable cementitious building materials must have compressive strength varying between 20 to 40 MPa.

3.7.2 Effect of GGBS in CDG

The influence of 5, 10 and 15% GGBS in volume in the fused CDG was also studied. In general, it can be observed that the increase of GGBS volume greatly improved the mechanical performance of the CDG geopolymer. Fused CDG with addition of 5, 10 and 15% GGBS cured with 24 hours heating first presents 32.09, 35.93 and 39.55 Mpa, respectively, at 28 days curing while cured at ambient temperature solely gives 21.44, 27.07 and 30.21 MPa, respectively. It is clear that compressive strength in this case also decreases when cured at ambient temperature over time compared to the mixtures heated at 70^{o}C for 24 hours. This is consistent with several studies that promoted ambient curing conditions by incorporating different supplementary materials such

as slag, calcium-rich fly ash, calcium hydroxide and OPC in order to increase geopolymerization reaction, minimize setting time and boost mechanical performance [42-48].

3.7.3 Split tensile strength development

Split strengths of the CDG are presented in Fig. 10 (b). It is apparent that split strength of the CDG is higher when temperature cured and fused mixture and with added GGBS. The split strengths of up to 0.84 and 0.39 were obtained, respectively, for the initial CDG cured with and without heating first for 24 hours. For the fused CDG, at the same curing conditions it reached a tensile strength of 1.95 and 0.98 MPa, respectively. The fused CDG mixtures with the three different volumes of added GGBS presented a strength of 2.75, 2.87 and 3.49 MPa, respectively, with the heating treatment, and 2.05, 2.23 and 2.62 MPa, respectively, for the mixtures without. From these results, it can be seen that the increase in the split strengths is directly related to the increase in compressive strength of the CDG geopolymer mortars. For strength development, it can deduce that the alkali fusion method adopted in this study has successfully changed the mineralogy of the CDG, increased Si and Al dissolution rate from the solid. It has also provided good mechanical performance after being cured under a short period of elevated temperature and even under normal temperatures solely.

3.8 Water durability and gel formation

To study water durability and to evaluate gel formation in the CDG geopolymer mortars, all the samples were immersed into water for 30 days and their respective water resistance was observed. Several studies have examined the sustainability of geopolymers with water resistance in alkali-activated aluminosilicate as one key parameter to access it [37, 49-51]. For example, Rees et al. [49] defined geopolymer as a material obtained by a mixture of alkali-metal, silica and alumina in water with high pH, which after transformation becomes a solid with high resistance to

514 water. In this study, a total of 10 samples composed of initial and fused CDG geopolymer mortars
515 with different curing conditions were immersed in water and their respective behaviors were
516 observed (Fig. 11). The samples composed of initial CDG showed some cracks, which propagated
517 slowly and dislocated over time (Fig. 11 b). This was after immersion in water after a few days.
518 The low resistance of these samples in water is due to low reactivity associated with its natural
519 state and crystallized phase of the CDG. Moreover, the low reactivity relates with its activation
520 with only sodium silicate (Na_2SiO_3) solution.

521 Moreover, the fused CDG and the CDG supplemented with GGBS showed no cracks on
522 their respective surfaces during the entirety of water immersion. Despite the 30 days of immersion
523 the samples of the mixtures kept their hardened and rigid appearance (Figs. 11 c-d), which can be
524 a proof of more reactive phase of the fused CDG and its success in the geopolymerization process.
525 Of note, some samples cured only at ambient temperature shown some cracks at their surface, but
526 most of them remained stable, solid and did not dislocate until after 30 days (Figs. 11 e-f). From
527 the foregoing, a deduction can be made that the binder is geopolymer and consists of the N–A–S–
528 H gel. Also, a conclusion can be drawn that geopolymerization reaction is mostly influenced by
529 the elevated temperatures. The origin of the cracks observed in the samples could be attributed to
530 the solubility phases induced by Na_2SiO_3 in the geopolymer matrix [52], a phenomenon relating
531 to the excess Na^+ free ions merged with the matrix that was combined soluble Si from the alkali
532 activator. The following equations illustrate sodium silicate gel solubility in water [53].

533 $$\equiv \text{Si-O} - \text{Na} + \text{H}_2\text{O} \rightarrow \equiv \text{Si-O-H} + \text{Na}^+\text{OH}^- \quad (1)$$

534 $$\equiv \text{Si-O-Si} \equiv + \text{OH}^- \rightarrow \equiv \text{Si-OH}^+ \equiv \text{Si-O}^- \quad (2)$$

535 $$\equiv \text{Si-OH} + \text{OH}^- \leftrightarrow \equiv \text{Si-O}^- + \text{H}_2\text{O} \quad (3)$$

536

Equation (1) defines the hydrolysis of silica gel bond (Si–O–Na) due to the development of silanol and hydroxyl groups. The reactions in Eq. (3) aids in raising the system pH and provides silica bond (–Si–O–Si–) hydrolysis as shown in Eq. 2 and 3. The low resistivity in water for the activated initial CDG samples is therefore related to the silica gel dissolution, constituting the main element of activation. This confirms, moreover, the low mechanical and physical properties observed on these samples, such as cracks propagation during the immersion tests and higher porosity detected by the SEM tests. From the aforementioned observations and considering the results obtained from the fused CDG, a conclusion can be drawn that alkali fusion aided CDG to be more active during the geopolymerization process and that the addition of GGBS into the fused CDG allows sufficient liberation of active Si^{4+} and Al^{3+}. Furthermore, the sustainability of geopolymers produced from fused source materials should be assessed using the water resistance test.

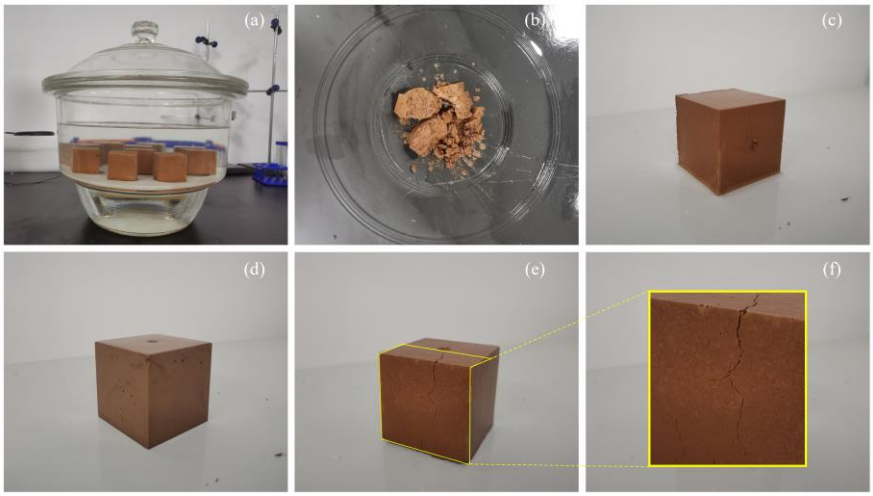

Fig. 11 Water resistance test: (a) Immersed samples, (b) dislocated initial CDG, (c) Fused CDG, (d) Fused CDG supplemented with GGBS, (e) Fused CDG cured at ambient temperature, (f) Cracks propagation

3.9 Potential applications of CDG

CDG, for some time now, has so far been considered as the raw material for filling in slopes retaining walls, excavations, foundations and subgrade works. These applications have not been

translated into large-scale, and the high-volume of CDG is associated with several environmental degradations. From the results obtained in this study, beside the benefits of fine contents of CDG proven by several researchers, its application in geopolymer technology has been made possible.

The recycling of CDG in the production of geopolymer can suitably contribute to its valorization and OPC use reduction, thereby helping municipalities in waste management. The results from the initial CDG presented a compressive strength reaching 4.75 and 8.89 MPa. This range of strength allows CDG applications for basic building materials and for components that do not require a high load resistance. The alkali fusion method adopted has helped to improve the mechanical properties of CDG. As a result, the fused CDG can offer strength between 16.99 and 27.65 MPa, which allows a wide range of applications in the building sector, as well as in pavement construction and low strength road structures. The addition of 5, 10 and 15% GGBS in volume into CDG gives, respectively, a strength of 21.44, 27.07 and 30.21 MPa if CDG geopolymer mortars are cured under ambient temperature, and revolves around 32.09, 35.93 and 39.55 MPa, respectively, if they are heat cured for 24 hours before curing in ambient temperature. The performance of CDG under these two different curing conditions, opens up opportunities for in-situ applications. This has made several advanced developments possible in areas such as precast industry, coatings for protecting reinforced concrete against corrosion. Composites for application in conservation, restoration and building decoration can all be tested to prove its real performance and applicability. The water resistance test also demonstrated the stability of the developed CDG geopolymers in water.

4. Conclusion

The possibility of recycling CDG waste by alkali fusion into geopolymer materials was investigated in this study. From the results obtained, the following conclusions can be drawn.

- CDG can be utilized as reactive aluminosilicate materials in the synthesis of geopolymer. The reactivity phase of CDG waste during alkali-activation is considerably upgraded by the adopted alkali fusion method.
- The dissolution of the initial CDG requires high molarity NaOH, while the fused CDG exhibits higher degree of dissolution at low NaOH concentration, a phenomenon that can be attributed to the addition of NaOH pellets during the alkali fusion process and the physico-chemical modifications of the released silica and alumina solid from the CDG in the presence of NaOH solution.
- The findings of the setting time showed that alkali fusion is very effective for heightening the dissolution of the fused CDG under Na_2SiO_3 solution. However, the setting time is inversely proportional to the degree of acceleration.
- Alkali fusion has a crucial effect on the functional group of CDG. The strong band observed in the initial CDG shifted to a lower wavenumber band for the fused CDG, a phenomenon associated with the stretching vibration of Si–O and Al–O groups. This indicates that the transformation from crystallized minerals to the formation of amorphous minerals.
- The microstructure characterization showed diversified structures with reduced pores and cracks, confirming the well-synthesized geopolymer structure. The alkalinity analysis demonstrated a good elemental concentration which allowed enough elements liberation in the network and high degree of synthesis.
- The resulting fused CDG with and without added GGBS, both reacted with sodium silicate solution to form a geopolymer binder that has the capacity to harden at room temperature or under moderate heating.

- The results of water resistance test confirmed that CDG geopolymers was mainly based on N–A–S–H gel and water resistance analysis was recommended as the key factor to access the sustainability of geopolymers produced from fused source materials. The strength of CDG geopolymer binders resulting from the initial, fused and fused with addition of GGBS is comparable to that of typical construction materials for specific applications.

In short, the application of CDG geopolymers can be diversified according to the characteristics studied. This study therefore provides a new recycling method of CDG into building materials and opens the way for further investigations on CDG especially on its mechanical and durability performance under alkali environments for its efficient and sustainable application as greener material, an alternative to Portland cement.

Further research relating to alkali/CDG mass ratio and molecular ratio of the activator are still required to improve the general properties of CDG for potential large-scale applications. Considering worldwide availability of CDG waste and the environmental consequences caused by its disposal, this study has proposed an effective recycling strategy that can be adopted by local municipalities and engineering enterprises to recycle CDG waste in the production of added value geopolymer materials, so as to limit waste disposal and the subsequently mitigate adverse environmental impact associated with CDG waste.

Declaration of competing interest

This study was not in any way affected by the financial interest or personal relationships of the authors that worked on this paper.

Acknowledgements

The authors gratefully acknowledge the support of National Nature Science Foundation of China (Grants No. 52008265, 52108233, No. 52078300, No. 51978414) and from the Royal Society, UK (IEC\NSFC\181449).

Data Availability Statement

This paper contains all data, models, and code created or employed during this study.

References

[1] Dassekpo, J.B.M, X.X. Zha, ., J.P. Zhan, Compressive strength performance of geopolymer paste derived from Completely Decomposed Granite (CDG) and partial fly ash replacement, Construction and Building Materials 138 (2017) 195-203.

[2] C. Wang, Q. Li, J. Zhu, W. Gao, X. Shan, J. Song, X. Ding, Formation of the 2015 Shenzhen landslide as observed by SAR shape-from-shading, Scientific Reports 7(1) (2017) 43351.

[3] B.o.H.a.U. Development, Shenzhen 2018 Annual Implementation Plan for Residual Waste Acceptance Site, in Chinese, 2018.

[4] Guide to Rock and Soil Descriptions, Geoguide 3, Geotechnical Engineering Office (GEO), Hong Kong, 1988.

[5] D. Kim, M. Sagong, Y. Lee, Effects of fine aggregate content on the mechanical properties of the compacted decomposed granitic soils, Construction and Building Materials 19(3) (2005) 189-196.

[6] Y.R. Zhao, Yang, H. Q., Huang, L. P., Chen, R., Chen, X. S., & Liu, S. Y., Mechanical behavior of intact completely decomposed granite soils along multi-stage loading–unloading path, Engineering Geology, 105242 (2019).

[7] S.Y. Wang, D. Chan, K.C. Lam, Experimental study of the effect of fines content on dynamic compaction grouting in completely decomposed granite of Hong Kong, Construction and Building Materials 23(3) (2009) 1249-1264.

[8] J. Davidovits, Geopolymers-inorganic polymeric new materials, Journal of Thermal Analysis 37(8) (1991) 1633-1656.

[9] J.L. Provis, Bernal, S.A., Geopolymers and related alkali-activated materials, Annu. Rev. Mater. Res. 44(299e327) (2014).

[10] K. Komnitsas, D. Zaharaki, Geopolymerisation: A review and prospects for the minerals industry, Minerals Engineering 20(14) (2007) 1261-1277.
[11] P. Duxson, Provis, J.L., Lukey, G.C., van Deventer, J.S.J., The role of inorganic polymer technology in the development of 'green concrete', Cement and Concrete Research 37, 1590–1597 (2007).
[12] C.L. Xianhui Zhao, Liming Zuo, Li Wang, QinZhu, Mengke Wang, Investigation into the effect of calcium on the existence form of geopolymerized gel product of fly ash based geopolymers, Cement and Concrete Composites 103 (2019) 279-292.
[13] C.L. Hongzhi Cui, Guochen Sang, Yu Jin, Zhijun Dong, Xiaohua Bao, Waiching Tang, Effect of carbon nanotubes on properties of alkali activated slag–A mechanistic study, Journal of Cleaner Production 245:119021 (2019).
[14] S.W. Sungwoong Yang, Jongki Lee, Hwayoung Lee, Sumin Kim, Biochar-red clay composites for energy efficiency as eco-friendly building materials: Thermal and mechanical performance, Journal of Hazardous Materials 373 (2019) 844-855.
[15] J.B.M. Dassekpo, J.Q. Ning, X.X. Zha, Potential solidification/stabilization of clay-waste using green geopolymer remediation technologies, Process Safety and Environmental Protection 117 (2018) 684-693.
[16] Dassekpo, J.B.M, Zha X. X, Zhan J. P, Synthesis reaction and compressive strength behavior of loess-fly ash based geopolymers for the development of sustainable green materials, Construction and Building Materials 141 (2017) 491-500.
[17] G. Medina, I.F.S. del Bosque, M. Frias, M.I.S. de Rojas, C. Medina, Durability of new recycled granite quarry dust-bearing cements, Construction and Building Materials 187 (2018) 414-425.
[18] D.H. L. Simão, M.J. Ribeiro, R.M. Novais, O.R.K. Montedo, F. Raupp-Pereira, Development of new geopolymers based on stone cutting waste, Construction and Building Materials 57:119525 (2020).
[19] Dassekpo, J.B.M., X.X. Zha, N.J. Q., Z.J. P, The effects of the sequential addition of synthesis parameters on the performance of alkali activated fly ash mortar, Results in Physics 7 (2017) 1506-1512.
[20] H. Xu, J.S.J. Van Deventer, The geopolymerisation of alumino-silicate minerals, International Journal of Mineral Processing 59(3) (2000) 247-266.

[21] H. Xu, L. Q, S. L, Z. M, Z. J, Low-reactive circulating fluidized bed combustion (CFBC) fly ashes as source material for geopolymer synthesis, Waste Management 30 (2010) 57–62 (2010).
[22] W.H.S. H.L. Chang, A general method for the conversion of fly ash into zeolites as ion exchangers for cesium, Industrial and Engineering Chemistry Research 37 (1998) 71–78. (1998).
[23] C.P. A. Molina, A comparative study using two methods to produce zeolite from fly ash, Minerals Engineering 17 (2004) 167–173. (2004).
[24] M.H. Shigemoto, H.; Miyaura, K. J., Selective formation of Na-X zeolite from coal fly ash by fusion with sodium hydroxide prior to hydrothermal reaction, Journal of Materials Science Volume 28, pages 4781–4786 (1993). (1993).
[25] J.N.Y.D. L.N. Tchadjié, N. Ranjbar, H.K. Tchakouté, B.B.D. Kenne, A. Elimbi, D. Njopwouo, Potential of using granite waste as raw material for geopolymer synthesis, Ceramics International 42, Issue 2, Part B (2015) 3046-3055.
[26] J.A.M. H.K. Tchakouté, A. Elimbi, B.B.D. Kenne, D. Njopwouo, Synthesis of volcanic ash-based geopolymer mortars by fusion method: effects of adding metakaolin to fused volcanic ash, Ceramic International 39 (2013) 1316–1321 (2013).
[27] J.B.M. Dassekpo, Feng W.P., Li Y.R., Miao L.X., Dong Z.J., Ye J.Q., , Synthesis and characterization of alkali-activated loess and its application as protective coating., Construction and Building Materials (May), 122631. (2021).
[28] X. Ke, Bernal, S.A., Ye, N., Provis, J.L., Yang, J., One-Part Geopolymers based on thermally treated red mud/NaOH blends, J. Am. Ceram. Soc. 98, 5e11. (2015).
[29] J.D. T.B. Douglas, Anhydrous sodium hydroxide: the heat content from 0o to 700oC, the transition temperature and the melting point, J. Res. Natl. Bur. Stand. 53 (1954) 81–90 (1954).
[30] N.W. Chen-Tan, van Riessen, A., LY, C.V., Southam, D.C., Determining the reactivity of a fly ash for production of geopolymers, Journal of the American Ceramic Society 92, 881–887 (2009).
[31] J.L. Provis, Duxson, P., van Deventer, J.S.J., Lukey, G.C.,, The role of mathematical modelling and gel chemistry in advancing geopolymer technology, Chemical Engineering Research and Design 83 (A7), 853–860 (2005).
[32] M. Handke, & Mozgawa, W. , Vibrational spectroscopy of the amorphous silicates, Vibrational Spectroscopy, 5(1), 75–84. (1993).

718 [33] W. Mozgawa, Sitarz, M., & Rokita, M., Spectroscopic studies of different aluminosilicate
719 structures, Journal of Molecular Structure, 511-512, 251–257. (1999).
720 [34] N. Schiavon, Kaolinisation of granite in an urban environment, Environmental Geology, 52(2),
721 399–407. (2006).
722 [35] D.W. Feng, J.L. Provis, J.S.J. van Deventer, Thermal Activation of Albite for the Synthesis
723 of One-Part Mix Geopolymers, Journal of the American Ceramic Society 95(2) (2012) 565-572.
724 [36] P. Tarte, Infra-red spectra of inorganic aluminates and characteristic vibrational frequencies
725 of AlO4 tetrahedra and AlO6 octahedra, Spectrochimica Acta Part A: Molecular Spectroscopy,
726 23(7), 2127–2143. (1967).
727 [37] G.H. A. Favier, J.B. d'Espinose de Lacaillerie, N. Roussel, Mechanical properties and
728 compositional heterogeneities of fresh geopolymer pastes, Cem. Concr. Res. 48 (2013) 9–16
729 (2013).
730 [38] A.M. Rashad, S.R. Zeedan, The effect of activator concentration on the residual strength of
731 alkali-activated fly ash pastes subjected to thermal load, Construction and Building Materials 25(7)
732 (2011) 3098-3107.
733 [39] J.S.J.v.D. W.K.W. Lee, The interface between natural siliceous aggregates and geopolymers,
734 Cem. Concr. Res. 34 (2004) 195–206 (2004).
735 [40] D.L.Y. Kong, J.G. Sanjayan, Damage behavior of geopolymer composites exposed to
736 elevated temperatures, Cement & Concrete Composites 30(10) (2008) 986-991.
737 [41] E.I. Diaz, E.N. Allouche, S. Eklund, Factors affecting the suitability of fly ash as source
738 material for geopolymers, Fuel 89(5) (2010) 992-996.
739 [42] G.M. Canfield, J. Eichler, K. Griffith, J.D. Hearn, The role of calcium in blended fly ash
740 geopolymers, Journal of Materials Science 49(17) (2014) 5922-5933.
741 [43] A. Palomo, A. Fernandez-Jimenez, G. Kovalchuk, L.M. Ordonez, M.C. Naranjo, Opc-fly ash
742 cementitious systems: study of gel binders produced during alkaline hydration, Journal of
743 Materials Science 42(9) (2007) 2958-2966.
744 [44] L. Assi, S. Ghahari, E. Deaver, D. Leaphart, P. Ziehl, Improvement of the early and final
745 compressive strength of fly ash-based geopolymer concrete at ambient conditions, Construction
746 and Building Materials 123 (2016) 806-813.

747 [45] A.A. Aliabdo, A.M. Abd Elmoaty, H.A. Salem, Effect of cement addition, solution resting
748 time and curing characteristics on fly ash based geopolymer concrete performance, Construction
749 and Building Materials 123 (2016) 581-593.
750 [46] P. Nath, P.K. Sarker, Use of OPC to improve setting and early strength properties of low
751 calcium fly ash geopolymer concrete cured at room temperature, Cement & Concrete Composites
752 55 (2015) 205-214.
753 [47] T. Suwan, M.Z. Fan, Influence of OPC replacement and manufacturing procedures on the
754 properties of self-cured geopolymer, Construction and Building Materials 73 (2014) 551-561.
755 [48] H.K. Shehab, A.S. Eisa, A.M. Wahba, Mechanical properties of fly ash based geopolymer
756 concrete with full and partial cement replacement, Construction and Building Materials 126 (2016)
757 560-565.
758 [49] C.A. Rees, J.L. Provis, G.C. Lukey, J.S.J. van Deventer, Attenuated total reflectance Fourier
759 transform infrared analysis of fly ash geopolymer gel aging, Langmuir 23(15) (2007) 8170-8179.
760 [50] J.L.P. A. Hajimohammadi, J.S.J. van Deventer, One-part geopolymer mixes from geothermal
761 silica and sodium aluminate, Ind. Eng. Chem. Res. 47 (2008) 9396–9405 (2008).
762 [51] C.P. I. Lancellotti, L. Barbieri, C. Leonelli, Alkali activation processes for incinerator residues
763 management, Waste Manag. 33 (2013) 1740–1749 (2013).
764 [52] U.F.C.M. P.N. Lemougna, M.P. Delplancke, H. Rahier, Influence of the chemical and
765 mineralogical composition on the reactivity of volcanic ashes during alkali activation, Ceram. Int.
766 40 (2014) 811–820 (2014).
767 [53] N.N. R. Redden, Microstructure, strength, and moisture stability of alkali activated glass
768 powder-based binders, Cem. Concr. Compos. 45 (2014) 46–56 (2014).